23rd International Conference on Renewable Energies and Power Quality (ICREPQ'25)
Tenerife (Spain), 25th to 27th June 20245
Renewable Energy and Power Quality Journal (RE&PQJ)
ISSN 2172-038 X, Volume No.23, September 2025

Experimental determination of the temperature coefficient of resistance of ACSR conductors using a radial conductor model

Ankit Soni[1,2], Jordi-Roger Riba[1] Manuel Moreno-Eguilaz[1], and Josep Sanllehí[2]

[1] Department of Electrical Engineering
AMBER High-Voltage Laboratory, Universitat Politècnica de Catalunya
Campus de Terrassa – 08222 Terrassa (Spain)
[2] SICAME Spain
C/ Albert Einstein 5 – 08635 Sant Esteve Sesrovires (Barcelona)

Abstract. Transmission conductors used in overhead power lines are typically helically stranded and often have a steel core to give the conductor mechanical strength and outer strands of aluminium or aluminium alloy to provide the current carrying capacity. The presence of a magnetic core has several effects on the behaviour of the conductors, such as the presence of an axial component of the magnetic field which interacts with the current of the different layers of conductive strands wound helically around the magnetic core. This has a major effect on the alternating current (AC) resistance of the conductor, which can be very different from the direct current (DC) resistance. When applying dynamic line rating (DLR) approaches, the surface temperature of the conductor is typically measured due to the inability to measure inside the conductor, but the average temperature determines the true value of the resistance. In this work, a thermal model of the conductor is used to account for the radial temperature distribution to more accurately determine the resistance of the conductor and the temperature coefficient of the resistance. The experimental results presented show the potential of the proposed method.

Key words. ACSR conductors, temperature resistance, DLR applications, AC resistance.

1. Introduction

To meet decarbonisation targets, there is a growing trend towards increased renewable energy generation and electrification. It is therefore of paramount importance to enable the efficient, safe and reliable operation of transmission and distribution lines [1], [2]. This growing demand for electrical energy inevitably leads to effective congestion of existing power lines, making it essential to optimise their capacity [3]. An attractive strategy for power line capacity optimisation is to apply DLR approaches, which are essentially based on adjusting the maximum current capacity (also known as ampacity) of the line according to the actual weather conditions [4], [5], which have a significant impact on the maximum capacity of the line, which in turn is determined by its thermal rating. Dynamic line rating is based on solving the conductor's heat balance equation and determining its weather-related maximum current capacity according to the actual weather conditions, so that a given conductor temperature is not exceeded [6].

Therefore, DLR approaches typically require on-line measurement of the surface temperature and the current flowing through the conductor using dedicated sensors, as well as the actual weather conditions (solar irradiance, air temperature, and wind parameters) [7], [8].

Aluminium conductor steel-reinforced (ACSR) conductors are widely used in transmission and distribution lines. These conductors consist of a core composed of galvanised steel strands used to increase the mechanical strength [9] surrounded by various layers of stranded aluminium or aluminium alloy strands wound in opposite directions, and used for current carrying purposes. Their thermal rating is essentially determined by their maximum permissible temperature [10], which in turn is determined by the sag they experience in high temperature operation. For ACSR conductors, this limit is typically around 80 ºC [11], as this temperature ensures safe clearances to earth and nearby conductors [10].

The main source of conductor heating is the internal power dissipation due to resistive losses, which increase with conductor temperature due to the positive value of the temperature coefficient of resistance. Therefore, it is very important to accurately determine such power losses when designing DLR approaches, and specifically the mean temperature of the conductor instead of the surface temperature and the temperature coefficient of the resistance. It should be emphasised that the conductor has a radial temperature gradient, since the inner strands are hotter than the surface, where radiative and convective cooling effects occur. However, this radial temperature distribution depends on several effects, including the laying ratio, the number of layers and the material of the strands, the magnitude of the current, and the air trapped between the strands [7].

Most of the available models ignore the radial temperature distribution [10], [12], [13], although this effect can have some impact, especially at high current densities [14], with differences of more than 10ºC reported in some cases [10], [14].

Using a thermal model of the conductor that accounts for the radial temperature distribution, and experimental measurements of the current passing through the conductor, this paper proposes a method to better

determine the average temperature of the conductor and the temperature coefficient of resistance, with the aim of obtaining an accurate prediction of the resistive losses in ACSR conductors.

The paper is organised as follows. Section 2 develops the characteristics of ACSR conductors. Section 3 gives full details of the experimental part. Section 4 presents and discusses the results obtained and finally section 5 concludes the paper.

2. The particularities of ACSR conductors

ACSR conductors belong to the family of steel reinforced conductors. The presence of a magnetic core gives these conductors a special behaviour. In such conductors, the AC resistance is not only temperature-dependent, as in conductors consisting only of aluminium or aluminium alloy strands, but also current-dependent. Because the aluminium wires are wound helically around the galvanised steel core, there is an axially distributed magnetic flux within the steel core, the strength of which increases with the magnitude of the current flowing through the conductor [10]. As the adjacent layers of aluminium wires are helically wound in opposite directions, their individual currents generate axial components of the magnetic field in opposite directions which tend to cancel each other out. Under AC excitation, the effect of the axial component of the magnetic flux is to induce hysteresis losses and eddy currents in the core, which in turn tend to alter the distribution of current density in the different aluminium layers. This effect is known as the transformer effect [9]. The magnitude of the axial component of the magnetic flux through the steel core depends on the intensity of the current passing through the conductor, the AC frequency, the lay length and the magnetic properties of the material of the steel core [15], the latter depending on its actual temperature and tensile stress [16]. Therefore, all the combined effect of all these parameters alters the value of the AC resistance of ACSR conductors [9], which is temperature and current dependent. It should be noted that due to the non-linear behaviour of the magnetic core, there are no valid formulations for determining the AC resistance of stranded conductors with magnetic core.

3. The experimental setup

This section describes the equipment and materials used in the laboratory experiments, including the ACSR conductors, sensors and instrumentation for measuring AC resistance, voltage drop and phase shift between voltage drop and current.

ACSR conductors have different AC resistance behaviour depending on the number of aluminium layers. The magnetic flux interaction between the aluminium layers and the steel core increases the AC resistance. Two-layer conductors experience significant axial flux cancellation, minimising the current dependency, while three-layer conductors have a low dependency and single-layer conductors have the highest dependency.

This paper examines the three-layer 550-AL1/71-ST1A conductor and the two-layer 135-AL1/22-ST1A conductor, the detailed parameters of which are given in Table I. A single-layer conductor was derived from the two-layer conductor by removing the outer aluminium layer. The three-layer version has a 7-strand steel core and 54 aluminium strands in three layers (7/54), while the two-layer version has a 7-strand steel core and 26 aluminium strands (7/26). The single layer version is 7/10.

Figure 1 shows the cross-section of the three-layer conductor (550-AL1/71-ST1A), the two-layer ACSR conductor (135-AL1/22-ST1A) and the single-layer conductor obtained by removing the last layer of the two-layer conductor.

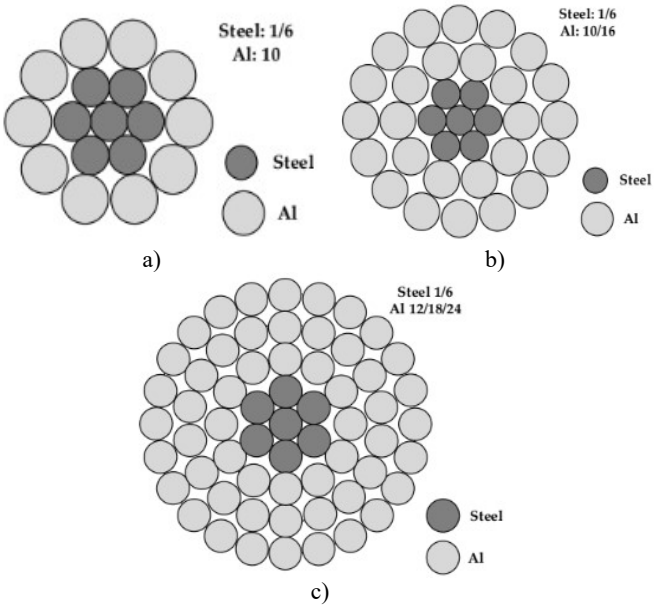

Figure 1. Cross Section Schematics of a). single layer b). two layer and, c). three layer conductor

Table I. Key parameters of two-layer (135Al/22-ST1A) and three-layer (550-AL1/71-ST1A) ACSR conductors

Symbol	Description	Three Layer	Two Layer	Unit
R_{20}	DC resist. at 20ºC	0.0526	0.2038	Ω/km
D	Conductor diameter	32.4	16.3	mm
D_{Al}	Aluminium wire diameter	3.6	2.57	mm
D_{steel}	Steel wire diameter	3.6	2	mm
N_{Al}	Number of aluminium wires	54 (12/18/24)	26 (10/16)	-
N_{steel}	Number of steel wires	7	7	-
A_{Al}	Area of aluminium	549.7	134.9	mm^2
A_{steel}	Area of steel	71.3	22	mm^2
m_{Al}	Al mass per unit length	1.5183	0.3717	kg/m
m_{steel}	Steel mass per unit length	0.5583	0.1728	kg/m

AC resistance and conductor temperature were measured under various laboratory conditions. A variable high current transformer (10 kVA, 380 V/4 V, output current: 0-2.5 kA, Transcir, Montcada i Reixac, Spain) was used to generate the required test current.

For analysis, the ACSR conductors were arranged in a low impedance circular loop connected to the high current transformer as shown in Figure 2. The conductor length used for the tests was 5.5 metres.

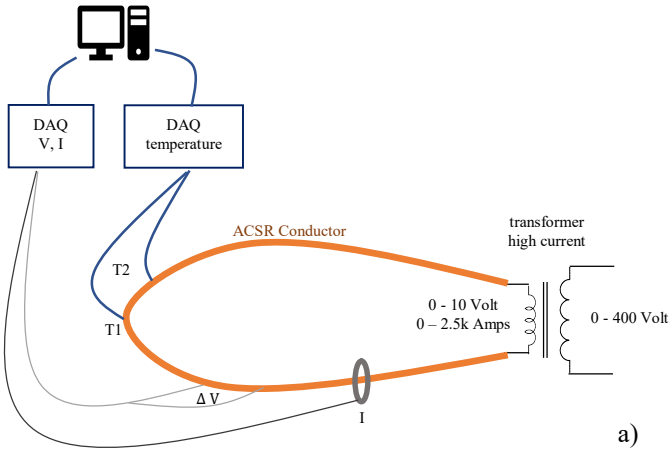

a)

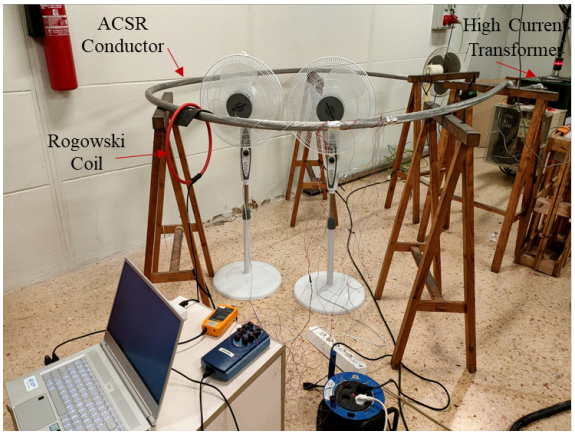

b)

Figure 2. Experimental setup for testing the ACSR conductors

Experimental tests carried out on ACSR conductor loops measured the current flowing through the loop, the voltage drop across a one metre length of conductor, the temperature at the surface of the conductor and the phase shift between the voltage drop and the current. Figure 2b shows a schematic of the experimental setup.

The current in the test loop was measured using an i3000s Flex Rogowski coil (sensitivity: 1 mV/A, Fluke Corporation, WA, USA) connected to an NI USB-6356 data acquisition system (National Instruments, Dallas, TX, USA) with a voltage accuracy of 564 microvolts.

Conductor surface temperatures were measured using T-type thermocouples (accuracy: ±0.8°C) connected to an OMB-DAQ-TC-RACK thermocouple input data acquisition system (accuracy: ±0.2°C, Omega, Hungary). Data acquisition from the OMB-DAQ-TC-RACK and NI USB-6356 systems was synchronised using custom Python code developed by the authors.

4. Results and discussion

Single-layer, two-layer, and three-layer ACSR conductors are being analysed for resistance variation with temperature. The surface temperature of the conductors and their AC resistance were measured at different current levels. Due to the presence of a steel core, the current level has a significant effect on the AC resistance, which prompted a detailed analysis for all three conductors under different conditions.

During these measurements, the temperature coefficient of resistance α was determined experimentally, providing a basis for its application in Dynamic Line Rating (DLR) models for conductor analysis. However, the temperature difference between the conductor surface and the core suggests that the actual α values may differ from the experimental results, and these adjusted values are referred to as α_{avg}.

To overcome this, an approach has been adopted to define the average alpha values by calculating the average conductor temperature using a simulation model. This model matches the surface temperature to the experimental values while estimating the temperature distribution across the radial direction of the conductor, which decreases from the core to the surface. Figure 3 shows the surface temperature (experimental and simulated), core temperature and average temperature for all three conductors, together with the variation in AC resistance as a function of conductor type and temperature.

Table II presents the results, highlighting the significant variation in alpha and average alpha values with changes in current. For the single-layer conductor, alpha increases from 0.00462 to approximately 0.005 as the current decreases from 220 Amps to 75 Amps. In contrast, for the two-layer conductor, alpha remains constant at 0.00351 across different current levels. For the three-layer conductor, alpha values are 0.00458 at 1020 A and 0.0047 at 310 A.

Table II. ACSR conductors. Comparison of the measured $\alpha_{surface}$ (measured) and α_{avg} (obtained with the radial model of the conductors).

Conductor Type	Current (A)	$\alpha_{surface}$ ($\times 10^{-3}$)	α_{avg} ($\times 10^{-3}$)
Single-layer conductor	220	4.62	4.52
	145	4.82	4.66
	75	5.09	4.84
Two-layer conductor	200 & 390	3.51	3.37
Three-layer conductor	1020	4.58	4.52
	310	4.7	4.62

The results also show that changes in the core and surface temperatures of the conductor result in reduced α_{avg} values. For the single-layer conductor, α_{avg} decreases from 0.00462 to about 0.00452 at 220 Amps and about 77ºC, from 0.00482 to 0.00466 at 145 Amps and almost 49ºC, and from 0.005 to 0.00484 at 75 Amps and 31.35ºC. The average temperature also deviates from the surface temperature by almost about 0.5 to 1.0ºC. In contrast, for the two-layer conductor, α_{avg} decreases from 0.00351 to 0.00337 for both 200 Amps (45ºC) and 390 Amps (87ºC). For the three-layer conductor, $\alpha_{surface}$ and α_{avg} shift from 0.00458 to 0.00452 at 1020 A (85ºC) and from 0.0047 to 0.00462 at 310 A (28ºC).

The results clearly show that different current levels have a significant effect on the total AC resistance and α values of a single-layer conductor. This effect is also observed in a three-layer conductor, whereas in a two-layer conductor the effect is negligible. In addition, the temperature difference between the core and the surface affects the α_{avg} coefficient, which could be used to develop more accurate models for Dynamic Line Rating (DLR) approaches.

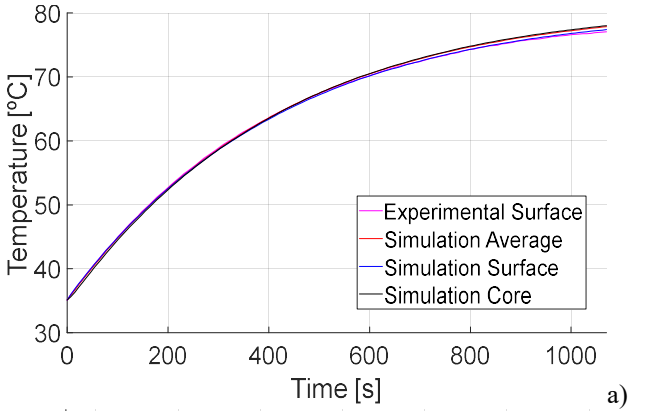

a)

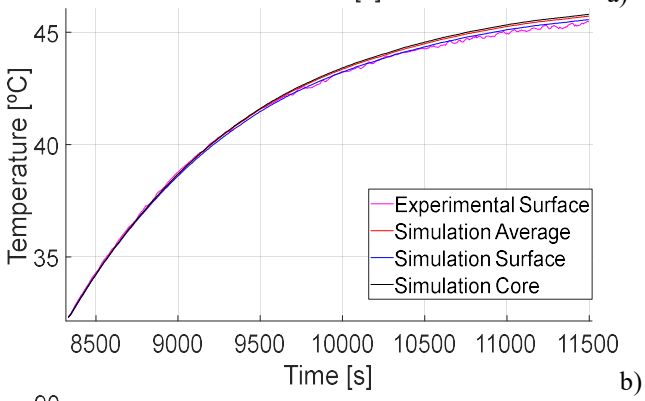

b)

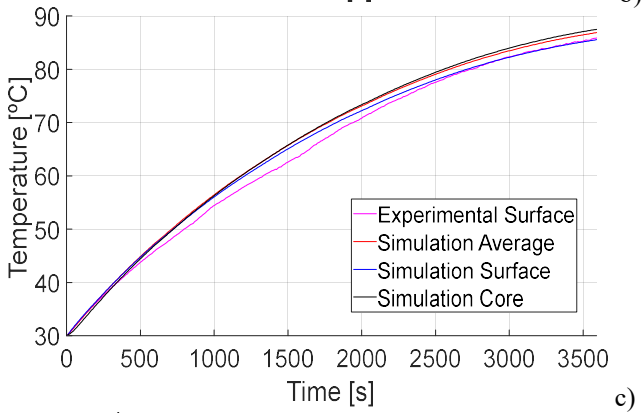

c)

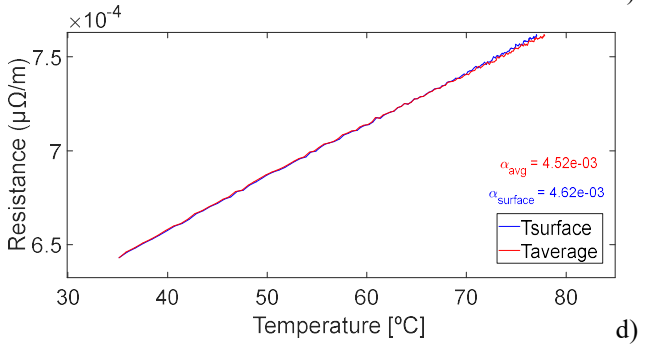

d)

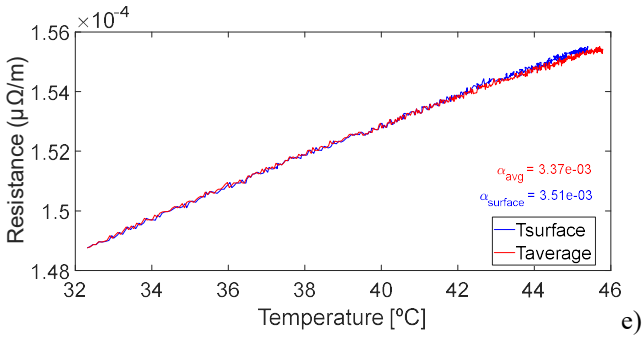

e)

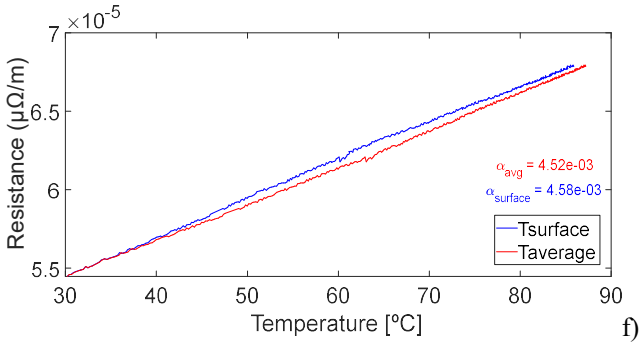

f)

Figure 3. Temperature change and temperature coefficient of resistance for single-, two-, and three-layer conductors. Subfigures 3a, 3b, and 3c show the surface, core, and average temperatures, while subfigures 3d, 3e, and 3f show the $\alpha_{surface}$ (experimental) and α_{avg} (simulated) values for single-, two-, and three-layers conductors respectively.

5. Conclusion

This paper has focused on a more accurate determination of the average temperature of ACSR conductors and its effect on the AC resistance, as resistive losses play a leading role in the development of thermal models of such conductors for Dynamic Line Rating (DLR) applications. It was explained that due to the complexity of stranded helically wound conductors with non-linear magnetic core, the AC resistance is not only temperature dependent but also current dependent, so that experimental results are required to better describe this phenomenon. Therefore, this combined effect makes it impractical to obtain exact formulae to determine the AC resistance of stranded conductors with a magnetic core.
The experimental results show significant variations in AC resistance and coefficient α for different conductor types and current levels. Although single-layer and three-layer conductors show a significant dependence on current, this effect is almost negligible for two-layer conductors. Furthermore, the temperature difference between the core and the surface causes deviations in the average temperature coefficient of resistance α_{avg}, demonstrating the importance of considering radial temperature distributions when modelling the behaviour of conductors.

The proposed thermal model, which aligns simulated and experimental surface temperatures and accounts for radial temperature gradients, provides a more accurate method for determining average conductor temperature and

resistance. This approach can improve the accuracy of DLR models by incorporating αavg values that reflect real world conditions. The results of this work will help to improve the thermal and electrical modelling of ACSR conductors, enabling more reliable and efficient use of transmission lines in dynamic operating environments.

Acknowledgement

This project received funding from grant PID2023-147016OB-I00,by MICIU/AEI/10.13039/501100011033/ and by ERDF "A way of making Europe," by the European Union and from the Agència de Gestió d'Ajuts Universitaris i de Recerca-AGAUR (2021 SGR 00392, 2024 DI 010).

References

[1] P. Castro, R. Lecuna, M. Manana, M. J. Martin, and D. Del Campo, "Infrared Temperature Measurement Sensors of Overhead Power Conductors," *Sensors 2020, Vol. 20, Page 7126*, vol. 20, no. 24, p. 7126, Dec. 2020, doi: 10.3390/S20247126.

[2] J.-R. Riba, Y. Liu, and M. Moreno-Eguilaz, "Analyzing the role of emissivity in stranded conductors for overhead power lines," *Int. J. Electr. Power Energy Syst.*, vol. 159, p. 110027, Aug. 2024, doi: 10.1016/J.IJEPES.2024.110027.

[3] R. S. Singh, S. Cobben, and V. Cuk, "PMU-Based Cable Temperature Monitoring and Thermal Assessment for Dynamic Line Rating," *IEEE Trans. Power Deliv.*, vol. 36, no. 3, pp. 1859–1868, Jun. 2021, doi: 10.1109/TPWRD.2020.3016717.

[4] R. Minguez, R. Martinez, M. Manana, D. Cuasante, and R. Garañeda, "Application of Digital Elevation Models to wind estimation for dynamic line rating," vol. 134, no. August 2021, p. 107338, Jan. 2022.

[5] A. Moradzadeh, M. Mohammadpourfard, I. Genc, Ş. S. Şeker, and B. Mohammadi-Ivatloo, "Deep learning-based cyber resilient dynamic line rating forecasting," *Int. J. Electr. Power Energy Syst.*, vol. 142, p. 108257, Nov. 2022, doi: 10.1016/J.IJEPES.2022.108257.

[6] J.-R. Riba, "The Role of AC Resistance of Bare Stranded Conductors for Developing Dynamic Line Rating Approaches," *Appl. Sci.*, vol. 14, no. 19, p. 8982, Oct. 2024, doi: 10.3390/APP14198982.

[7] J.-R. Riba, "Radial Thermoelectric Model for Stranded Transmission Line Conductors," *Sensors*, vol. 23, no. November 2023, pp. 1–19, 2023, doi: 10.3390/s23229205.

[8] S. Bustamante *et al.*, "Thermal behaviour of medium-voltage underground cables under high-load operating conditions," *Appl. Therm. Eng.*, vol. 156, pp. 444–452, Jun. 2019, doi: 10.1016/J.APPLTHERMALENG.2019.04.083.

[9] Cigré 345, "Alternating current (AC) resistance of helically stranded conductors." Cigré, Paris, pp. 1–59, 2008.

[10] IEEE Std 738-2012, "IEEE Standard for Calculating the Current-Temperature of Bare Overhead Conductors," New York, USA, 2012. doi: 10.1109/IEEESTD.2013.6692858.

[11] Y. Liu, J.-R. Riba, M. Moreno-Eguilaz, and J. Sanllehí, "Analysis of a Smart Sensor Based Solution for Smart Grids Real-Time Dynamic Thermal Line Rating," *Sensors 2021, Vol. 21, Page 7388*, vol. 21, no. 21, p. 7388, Nov. 2021, doi: 10.3390/S21217388.

[12] Cigré Working Group 22.12, "Thermal behaviour of overhead conductors," Cigré, Paris (France), 2002. [Online]. Available: https://e-cigre.org/publication/207-thermal-behaviour-of-overhead-conductors

[13] International Electrotechnical Commission and IEC, "IEC TR 61597:2021 Overhead electrical conductors - Calculation methods for stranded bare conductors," IEC, Geneva, Switzerland, 2021. Accessed: Oct. 27, 2021. [Online]. Available: https://webstore.iec.ch/publication/61412

[14] D. Douglass, "Radial and axial temperature gradients in bare stranded conductor," *IEEE Trans. Power Deliv.*, vol. 1, no. 2, pp. 7–15, 1986, doi: 10.1109/TPWRD.1986.4307928.

[15] B. S. Howington, L. S. Rathbun, D. A. Douglass, and L. A. Kirkpatrick, "AC resistance of ACSR — magnetic and temperature effects," *IEEE Trans. Power Appar. Syst.*, vol. PAS-104, no. 6, pp. 1578–1584, 1985, doi: 10.1109/TPAS.1985.319175.

[16] R. A. Meyberg, F. M. Absi Salas, L. A. M. C. Domingues, M. T. Correia de Barros, and A. C. S. Lima, "Experimental study on the transformer effect in an ACSR cable," *Int. J. Electr. Power Energy Syst.*, vol. 119, p. 105861, Jul. 2020, doi: 10.1016/J.IJEPES.2020.105861.

[17] IEC, "IEC 60287-1-1:2023. Electric cables - Calculation of the current rating - Part 1-1: Current rating equations (100 % load factor) and calculation of losses - General." IEC, Geneva, Switzerland, p. 38, 2023. [Online]. Available: https://webstore.iec.ch/publication/68118

[18] T. A. Association, *Aluminum Electrical Conductor Handbook*, Third. Washington DC, USA, USA: The Aluminum Association, 1989. Accessed: May 12, 2024. [Online]. Available: https://www.aluminum.org/aluminum-electrical-conductor-handbook